Geodesy and Geodynamics 2013,4(1):41 -45

http://www.jgg09.com
Doi:10.3724/SP.J.1246.2013.01041

Application of a simultaneous iterations reconstruction technique for a 3-D water vapor tomography system

Wang Wei[1], Ye Biwen[1] and Wang Jiexian[2]

[1] *Earthquake Administration of Jiangsu Province, Nanjing* 210014, *China*

[2] *College of Surveying and Geo-informatics, Tongji University, Shanghai* 200092, *China*

Abstract: The simultaneous iterations reconstruction technique (SIRT) is one of several reconstruction algorithms of the ART family. It is used widely in tomography because of its convenience in dealing with large sparse matrices. Its theoretical background and iteration model are discussed at the beginning of this paper. Then, the implementation of the SIRT to reconstruct the three-dimensional distribution of water vapor by simulation is discussed. The results show that the SIRT can function effectively in water vapor tomography, obtain rapid convergence, and be implemented more easily than inversion.

Key words: SIRT; reconstruction; water vapor; tomography; iteration

1 Introduction

The signals transmitted from Global Navigation Satellite Systems (GNSS) to receivers usually involve path delays when they cross the troposphere due to neutral atmosphere refraction. Recently, much research on the tomographic reconstruction of tropospheric water vapor using signal delays has been carried out, and the results have been used for short-term weather forecasting and disaster monitoring. Due to variations in the atmosphere, particularly the uncertainty in the spatial distribution of water vapor, the development of high-precision positioning is limited, though GNSS tomography can provide good estimates of the distribution of water vapor, which should benefit atmospheric correction in navigation and positioning.

However, water vapor tomography is affected by observational conditions. The method of solving normal equations can be generally summarized by the following three aspects.

1) In an ideal situation, there is at least one station in each grid cell observed from the horizontal plane. The inversion of a normal equation can be performed directly. However, it is difficult to satisfy this situation using the existing GNSS network.

2) The distribution of slant paths is inhomogeneous in the atmosphere because of the bad geometry of the GNSS network, which eventually leads to a cluster of slant delays in some grid cells. Then, the singular value decomposition technique [1] computes the eigenvalues of the system and identifies the null space of the solution, characterized by zero eigenvalues. The inversion of the overdetermined part can be performed directly [2].

3) The constraint equations not only provide information but also stabilize the normal equation. However, the variety of observations increases the difficulty of least-square inversion and prior weighting. The Kalman filter algorithm [3] can circumvent these limitations [4]; however, the initial value of the state vector and the variance-covariance matrix are difficult to determine.

In recent years, the algebraic reconstruction technique has been continually used in tomographic recon-

Received:2012-12-16; Accepted:2013-1-30

Corresponding author: Wang Wei, E-mail: wangwei_nj@126.com

This work is supported by the National Natural Science Foundation of China(40974018), National 863 Plan Projects(2009AA12Z307).

struction. This method provides fast algorithms that lead to stable results without many iterations [5]. The simultaneous iterative reconstruction technique (SIRT) is one such method. It has been increasingly applied in ionospheric tomographic reconstruction due to its convenience of use [6,7]. The SIRT is not the same type of iteration method as the ART, which estimates a correction for each grid cell and adds this term to the preceding value. The SIRT evaluates only one correction term for each grid cell that considers all observations. The correction term is therefore independent on the order of the constant vector. In this way, the efficiency and precision are both improved. This study focuses mainly on the application of the SIRT in troposphere tomography to reduce the computation time and increase the efficiency of near-real weather forecasting and disaster monitoring.

2 The theory of water vapor tomography

It is assumed that the distribution of water vapor in each grid cell is homogeneous during a short period. When a GPS signal crosses the atmosphere, it is cut into several lines by supposed grid cells in the atmosphere; thus, the observation equation [8] can be described by

$$\sum a_{i,j,k}x_{i,j,k} = swv \tag{1}$$

The matrix form is

$$\boldsymbol{AX} = \boldsymbol{SWV} \tag{2}$$

where $\boldsymbol{A}$ is the coefficient matrix with all intercepts crossing the grid cells, $\boldsymbol{X}$ is the unknown parameter vector that represents water vapor, and $\boldsymbol{SWV}$ is a constant vector whose components represent the total water vapor along a slant path. Due to the large number of grid cells and the nonuniform distribution of observations, some grid cells will not be covered. To resolve this problem, horizontal and vertical constraint equations are introduced. The tomography model is as follows:

$$\begin{pmatrix} SWV \\ 0 \\ 0 \end{pmatrix} = \begin{pmatrix} A \\ H \\ V \end{pmatrix} X + \begin{pmatrix} \Delta_1 \\ \Delta_2 \\ \Delta_3 \end{pmatrix} \tag{3}$$

where $\boldsymbol{H}$ and $\boldsymbol{V}$ are the horizontal and vertical coefficients, respectively.

3 The simultaneous iterative reconstruction technique

The SIRT is, in some ways, an improvement of the ART. It evaluates only one correction term for each grid cell that considers all observations. The correction term is therefore independent of the order of the constant vector [9,10]. The iteration can be described by

$$x_j^{k+1} = x_j^k + \sum_{i=1}^{m} \lambda a_{ij} \frac{swv_i - \sum_{j=1}^{n} a_{ij}x_j^k}{\sum_{j=1}^{n} a_{ij}^2} \tag{4}$$

where x is the water vapor parameter, m is the row number of observation functions, n is the column number and also the number of parameters, a_{ij} indicates the factor in row i and column j of the coefficient matrix, swv represents the observation data, and λ is the relaxation parameter.

SIRT algorithms require several iterations to reach convergence. Usually, the criteria are defined to be small in number, which allows for the optimal termination of the iteration. Another way is based on the criterion $|SWV_0 - AX^k| = \min$, which is satisfied by computing SWV using equation (3). However, this criterion is difficult to realize for water vapor tomography by the pattern of convergence described above. In this study, we introduced the variance of Mean difference and root-mean square as the termination criteria. Because each procedure can obtain increasingly accurate results with the increase in the number of iterations if it is convergent, the algorithm will terminate after a small number of iterations ($\xi < 10^{-6}$).

Mean difference ($mdif$)

$$mdif = \frac{1}{m}\sum_{i=1}^{m}(swv_i^k - swv_i^0) \tag{5}$$

Root-mean square (*rms*)

$$rms = \sqrt{\frac{1}{m-1}\sum_{i=1}^{m}(swv_i^k - swv_i^0 - mdif)^2} \quad (6)$$

The initial water vapor value in each grid cell can be determined by as follows: 1) interpolate the meteorological elements; 2) use the standard meteorological elements, which is not a very accurate method but is easy to implement; 3) introduce a numerical forecasting model (i.e., NCEP/ECMWF/MM5), which can provide data regarding pressure, temperature, humidity etc. with high precision.

4 Numerical simulation experiment

4.1 Over view of experiment

A numerical simulation experiment based on the Shanghai GPS monitoring network was carried out to test and verify the feasibility of water vapor tomography by the SIRT algorithm. The study region stretches across a horizontal distance of 0.6° and a vertical height of 10 km. It is divided into four parts along the east-west direction and north-south direction, with 20 layers along the vertical direction. The total number of grid cells was 320. There are nine GPS stations homogeneously distributed in the plane region (Fig. 1). Data gathered on September 13th UTC 00 : 00 – 00 : 30 from the Shanghai GPS monitoring network were processed operationally; the main process can be divided into the following four steps.

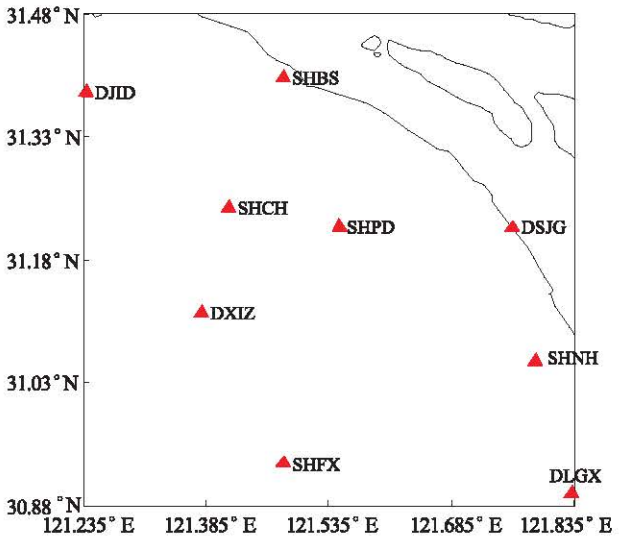

Figure 1 The distribution of Shanghai GPS network

1) Coefficient matrix of observation equation. Signals from the GPS to receivers traverse the atmosphere and produce intercepts in grid cells, which form the coefficient matrix $\boldsymbol{A}$.

2) Simulation observations. The European Centre for Medium Range Weather Forecasts (ECMWF) provides meteorological elements of the global atmosphere, such as pressure, temperature, specific humidity, etc., in a grid pattern. The simulated *swv* can be obtained in two steps. First, the ECMWF elements are interpolated along slant paths in the research region. Second, swv_s can be described as the integration of pressure, temperature, and vapor pressure obtained from the first step. In reality, observation is affected by white noise; thus, we add some random errors to swv_s.

$$swv_r = swv_s + e \quad (7)$$

3) Parameter of interest. The water vapor of the grid cells is considered the parameter of interest, which should be computed by equation (4). The initial values of the water vapor can be calculated using meteorology files.

4) Owing to the inhomogeneous distribution of slant observations, horizontal and vertical constraints are introduced.

4.2 Algorithm experiment and analysis

The relaxation parameter is one of the key factors that determines the convergence of the algorithm; therefore, the value should be chosen properly. In our study, an optimal search strategy was adopted using stop criteria for which the mean difference (MDIF) and root-mean square (RMS) would converge during iteration. As figure 2 shows, the data range is from 0 to 1, and the search step is 0.01. When λ is added to 0.12, the iteration converges; meanwhile, MDIF and RMS decrease and finally reach their minima. Otherwise, the iteration diverges. In this case, the optimal value of λ is 0.12. After determining the relaxation parameter, the efficiency of the iteration should be analyzed.

Figure 3 shows that the SIRT converges rapidly. The convergence speed of MDIF is faster than that of RMS. The former tends toward stability after 10 iterations, while the latter requires 100 iterations. The stability values for MDIF and RMS are 0.09 mm and 1.57 mm, respectively.

To determine the tomography quality, we compared the iterated water vapor with the ECMWF elements. A satisfactory vertical profile of water vapor was obtained from the SIRT algorithm, as shown in figure 4. The figure 4 shows that the variation trends of the two profiles are the same, with only a slight difference in values. Below a height of 5.5 km, the tomography values are slightly lower than the ECMWF values, whereas above 5.5 km, the tomography values are slightly higher

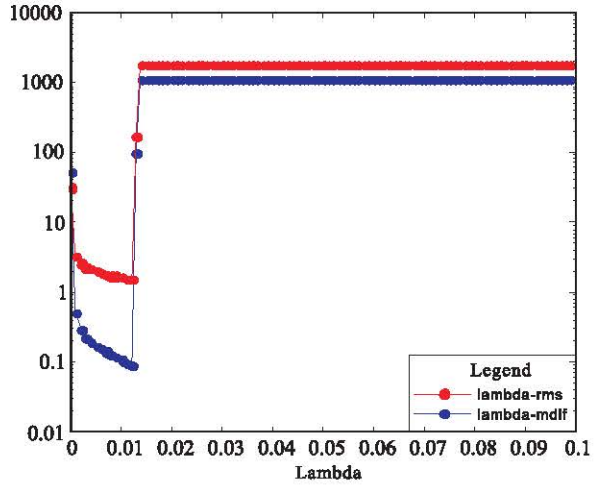

Figure 2 Quality of the reconstruction for different values of the relaxation parameter

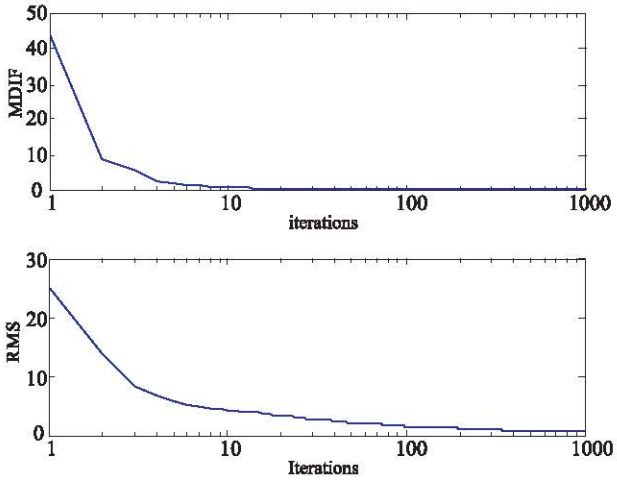

Figure 3 Convergence of SIRT algorithm

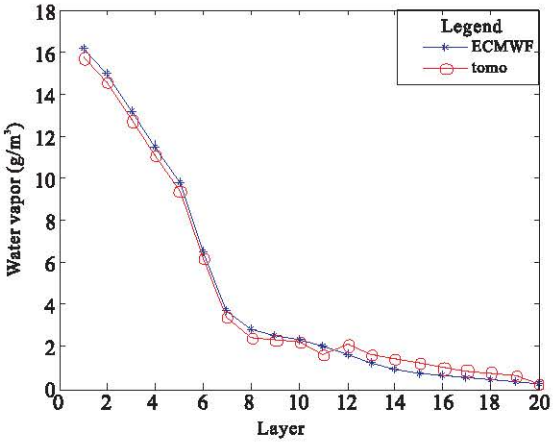

Figure 4 Vertical profile of tomography and water vapor from ECMWF

than the ECMWF values. Figure 5 shows the tomographic reconstruction profile maps, which correspond to the specified latitudes from west to east. The distribution of water vapor is correctly expressed by the profile maps. As shown, most of the vapor is clustered within a height of 3 km from the ground, decreasing with height. At a height of 10 km, the amount water vapor is close to zero. Some defects are observed in the profile map of $B = 31.18°$, which indicate that the SIRT algorithm exhibits some deficiencies.

5 Conclusions

1) The relaxation parameter is the weight of corrections. It is very important because it affects the efficiency and quality of iteration. In this study, λ spanned from 0.01 to 0.12, and the optimal value was 0.12.

2) The SIRT algorithm relies on an initial value. A proper initial value can not only improve the iteration efficiency but also produce an accurate result in the case of inhomogeneous observation distributions.

3) MDIF and RMS are considered to be the stop criteria. They converge to small values after 100 iterations. Because the SIRT uses a full correction strategy, an excessive number of iterations will induce individual deviations, although the results improve with the increasing number of iterations.

Overall, the tomography process is influenced by various factors. Moreover, the SIRT algorithm should be improved in future studies.

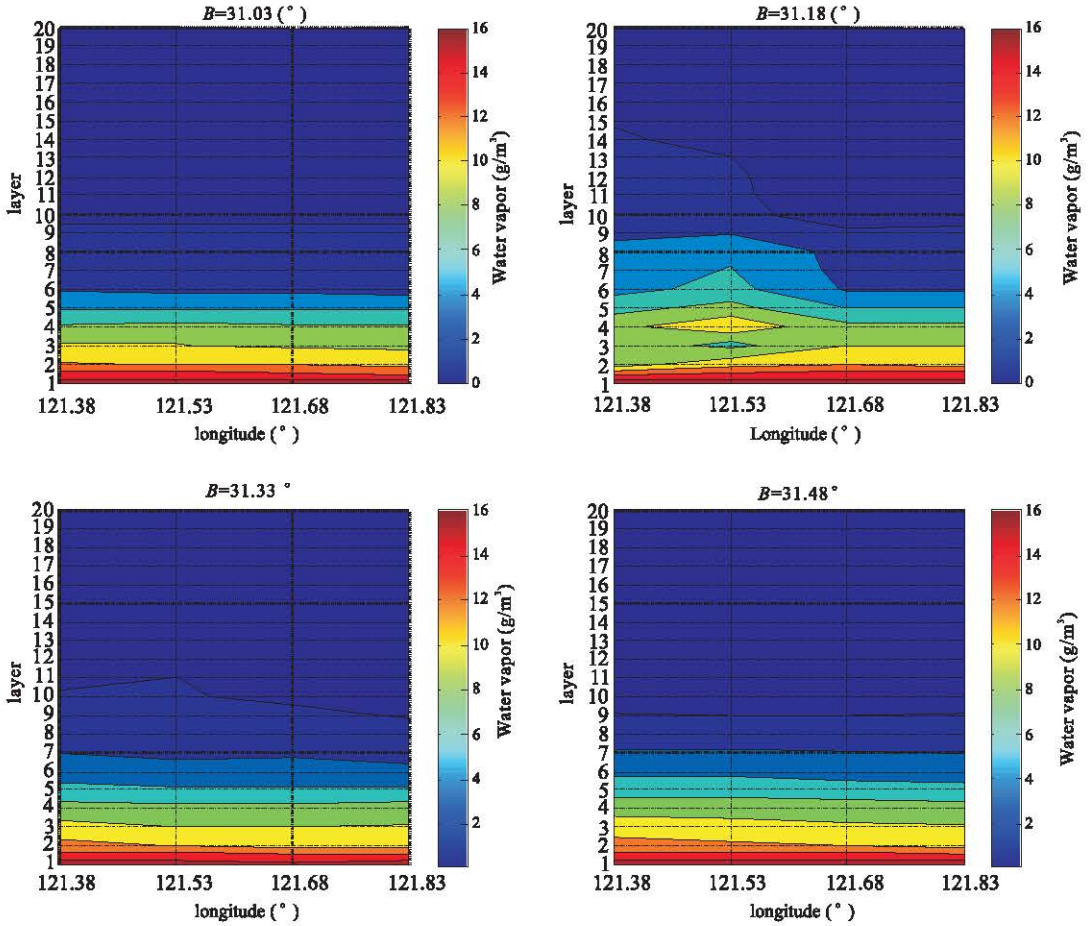

Figure 5 Tomographic reconstruction profile maps

Acknowledgements:

I'm particularly grateful to Associate Professor Song Shuli and Professor Zhu Wenyao for their help in my research.

References

[1] Flores A, Rius A, and Ruffini G. 4D tropospheric tomography using GPS slant wet delays, Ann. Geophys., 2000, 18:223 – 224.

[2] Miidla P, Rannat K and Uba P. Tomographic approach for tropospheric water vapor detection. Computational Methods in Applied Mathematics, 2008,(8): 263 –278.

[3] Lubomir P, Grandinarsky and Per Jarlemark. Ground-based GPS tomography of water vapor: analysis of simulated and real data. Journal of the Meteorological Society of Japan, 2004, 82:551 – 560.

[4] Zhang Shuangcheng, Ye Shirong, Wan Rong and Chen Bo. Preliminary tomography special wet refractivity distribution based on kalman filter. Geomatics and Information Science of Wuhan University, 2008, 8(8):798 – 802 (in Chinese).

[5] Stolle C, Schlüter S, Heise S, Jacobi Ch, Jakowski N and Raabe A. A GPS based three-dimensional ionospheric imaging tool: Process and assessment. J Adv Space Res., 2006, 38 (11): 2313 – 2317.

[6] Wen Debao, Liu Sanzhi and Tang Pingying. Tomographic reconstruction of ionospheric electron density based on constrained algebraic reconstruction technique. J GPS Solut., 2010, doi: 10.1007/s10291-010-0161-0.

[7] Sanzhi Liu, et al. Inversion of ionosphere electron density based on a constrained simultaneous iteration reconstruction technique. IEEE Transactions on Geoscience and Remote Sensing, 2010, 48:2455 –2459.

[8] Song Shuli, et al. Water vapor tomography from GPS data and it's application in improving numberical weather forecast. J Science Bulletin. ,2005,(20):2271 –2277.

[9] Bust G S and C N Mitchell. History, current state, and future directions of ionospheric imaging. Rev Geophys., 2008, 46, RG1003, doi:10.1029/2006RG000212.

[10] Heise S, et al. Integrated water vapor from IGS ground-based GPS observations: initial results from a global 5-min data set. Ann Geophys., 2009,27:2851 –2859.